JOURNAL OF SCIENCE TECHNOLOGY AND EDUCATION 13(1), MARCH, 2025
ISSN: 2277-0011; Journal homepage: www.atbuftejoste.com.ng

Effect of Rice Husk and Sugarcane Bagasse Pore Formers on the Microstructural Properties of Kaolin Ceramic

[1]Yusuf Tijjani, [2]Abubakar Muhammad Shitu
[1]*Department of Mechanical Engineering, Bayero University Kano, Kano State, Nigeria*
[2]*Department of Mechanical Engineering, Binyaminu Usman Polytechnic, Hadejia, Jigawa State, Nigeria*

ABSTRACT

Nigeria is endowed with diverse mineral resources, featuring over 40 deposits at over 450 sites. However, a considerable number of these, like kaolin, lack economic viability. The substitution of synthetic ceramic materials (e.g., Al2O3, ZrO2, SiC, TiO2) with locally sourced materials like Gwarzo kaolin can potentially improve the viability and utilization prospects of these domestic resources. This study investigates the effect of Agro-waste; rice husk (RH) and sugarcane bagasse (SCB) on the microstructural properties of Gwarzo kaolin. The locally sourced kaolin, RH and SCB were used in the production of ceramic samples by pore-forming agent (PFA) method, which involves addition of RH and SCB in the ceramics, followed by burning out the pore formers to obtain the porous ceramics. The Porosities, Densities, Average pore sizes of the RH and SCB graded samples were investigated. The average pore size diameter of samples with 3%wt, 6%wt, 9%wt RH was found to be 14.45µm, 16.33µm, 20.32µm respectively while 16.33 µm, 22.88 µm and 49.24µm for the same weight percentages of SCB. The findings reveal that both RH and SCB significantly influence the microstructural properties, in different ways. SCB leads to the formation of a more porous ceramics, whereas RH produces ceramics with lower porosity. The porosity and pore diameter measurements indicate that Gwarzo kaolin is a promising material for manufacturing macro-filters, which could be utilized in the initial stages of water treatment. Depending on the desired porosity, either RH or SCB can serve as effective pore former.

ARTICLE INFO
Article History
Received: November, 2024
Received in revised form: December, 2024
Accepted: January, 2025
Published online: March, 2025

KEYWORDS
Rice husk (RH), Sugarcane bagasse (SCB), Porous kaolin ceramic, Microstructural properties, Sustainability

INTRODUCTION

Rice husk (or rice hulls) is the hard protecting coverings of grains of rice. It is a major waste product of the rice milling from rice milling industries, which is a cellulose-based fiber and contains approximately 20% silica in amorphous form (Phonphuak & Chindaprasirt, 2015). Furthermore, it consists of 60–65% volatile matter, 10–15% fixed carbon, and 17–23% ash (Christophe *et al.,* 2017). It contains approximately 40% cellulose, 30% lignin group, and 20% silica (Chindaprasirt *et al.,* 2007). Rice husk (RH) can absorb water ranging from 5% to 16% of unit weights, and the unit weight of RH is 83–125 kg/m^3 (Phonphuak & Chindaprasirt, 2015). Research by Mohanta *et al.* (2014) and Wei *et al.* (2010) demonstrates the use of RH as a pore former in ceramic production. Mohanta *et al.* (2014) varied RH particle size and content, achieving ultra-high porosity (20-66vol%) and hierarchical pore structures. Wei *et al.* (2010) utilized RH to create porous cordierite ceramics with 42.4-45.02vol% porosity, leveraging its dual role as a pore former and silica source.

Sugarcane bagasse (SCB) is the fibrous residue left after extracting juice from sugarcane. For every 10 tonnes of sugarcane processed, around 3 tonnes of wet bagasse are produced. Although large-scale sugar factories are scarce in Nigeria, bagasse is plentiful due to local

Corresponding author: Yusuf Tijjani
ytijjani.mec@buk.edu.ng
Department of Mechanical Engineering, Bayero University Kano, Kano State, Nigeria.

JOURNAL OF SCIENCE TECHNOLOGY AND EDUCATION 13(1), MARCH, 2025
ISSN: 2277-0011; Journal homepage: www.atbuftejoste.com.ng

sugarcane consumption. Bagasse is primarily composed of cellulose, with its content varying based on sugarcane type and harvesting method. Notably, "Energy Cane" - a variety with lower sucrose but higher fiber content - has gained attention for its potential efficiency in fiber production (Haghdan *et al., 2016*).

Porous ceramics have gained significant attention in recent years due to their versatility and potential for various industrial applications, including filtration, fuel cells, catalysis, insulation, biomedical scaffolds, and more (Li and Li, 2012; Ohji and Fukushima, 2012; Ren *et al.,* 2013; Roohani-Esfahani *et al.,* 2013). Ceramic membranes are thermally and chemically stable porous materials widely used in separation processes like microfiltration and ultrafiltration, serving key industries including chemical, food, and textile sectors (Ali *et al.,* 2018; Saini *et al*., 2019; Aissat *et al.,* 2019; Abdullayev *et al.,* 2019). Alumina is often applied as a layer on ceramic supports due to its stability, filtration capabilities, and potential to reduce costs by minimizing the use of expensive materials (Zou *et al.,* 2024).

The high production costs of commercial ceramic membranes can be primarily attributed to the expense of conventional raw materials and the significant energy requirements associated with the sintering process. Besides alumina, zirconia, titania, and silica are also commonly used (Souza *et al.,* 2021), but they require high sintering temperatures (1500–1800 °C) (Dhuban *et al.,* 2019; Yang *et al.,* 2020), resulting in significant energy usage. Natural materials such as kaolin and common clay provide an economical and sustainable alternative, leveraging their abundance, low cost, and favorable properties like plasticity to reduce sintering temperatures and enhance processability (Lima *et al.,* 2024; Kamoun *et al.,* 2020).

Using Agro-waste materials as pore formers or structuring agents in ceramics is a smart way to repurpose potential pollutants, reducing waste and promoting sustainability (Li *et al.,* 2020; Xavier *et al.,* 2022; Hubadillah *et al.,* 2020). The utilization of locally available and abundant raw materials, such as RH, SCB, and Gwarzo's kaolinitic clays, is vital for developing cost-effective and environmentally sustainable technologies.

While previous research has explored using RH and SCB in ceramic production (Dele-Afolabi et al., 2018; Dele-Afolabi et al., 2022), our study uniquely investigates the combined use of raw RH and SCB with locally sourced kaolinitic clays from Gwarzo, Nigeria, to determine the microstructural properties of porous ceramic substrates.

MATERIALS AND METHODS

Materials

The raw materials used in this research were sourced from various locations in Nigeria. Specifically:

a. Kaolin clay was obtained from Gwarzo Local Government, Kano State.
b. Rice husk was sourced from a rice mill in Hadejia, Jigawa State.
c. Bentonite clay was procured from Maiduguri, Borno State.
d. Sugarcane bagasse was acquired from Hadejia market, Jigawa State.

Methods

Kaolin Beneficiation/ Preparation of Kaolin Powder

The kaolin clay sourced from Gwarzo quarry, Kano State, was processed through a series of steps. Initially, the clay was ground into powder using a ball mill (Keresoesterberg Overveld No. 057748) at 200 rpm for 2 hours. The powder was then soaked in water for 24 hours, allowing for the separation of insoluble particles from the soluble portion. After settling for 3 days, the supernatant water was decanted, and the resulting kaolin slurry was oven-dried at 150°C for 8 hours. The dried kaolin was reground into powder and subsequently calcined in a blast furnace (Nabertherm LH 120/14) at 700°C for 2 hours to remove volatile impurities and water (Zewdie *et al*., 2021). The final product was a refined kaolin powder. The Figure 1 below shows the flow diagram for the various stages in the beneficiation/ Preparation of Kaolin Powder.

Corresponding author: Yusuf Tijjani
ytijjani.mec@buk.edu.ng
Department of Mechanical Engineering, Bayero University Kano, Kano State, Nigeria.

JOURNAL OF SCIENCE TECHNOLOGY AND EDUCATION 13(1), MARCH, 2025
ISSN: 2277-0011; Journal homepage: www.atbuftejoste.com.ng

Figure 1: The block diagram for beneficiation/ Preparation of Kaolin Powder.

X-Ray Fluorescence (XRF) Analysis

The oxide composition of the sample was determined using XRF analysis. Prior to analysis, the sample cup was cleaned and fitted with a filter, and the sample was placed in the cup to a thickness of at least 3 mm, covering the filter. The instrument was allowed to warm up for 30 minutes before selecting the appropriate analysis method based on the sample's nature and objective. The sample was then labeled and positioned for measurement. Upon initiating the analysis, the instrument rotated the sample to the X-ray position, and the measurement was completed within 6-7 minutes. The resulting intensities were converted to concentrations (mg/cm^3). The analysis was conducted in accordance with ISO 12677:2011, and the results are presented in Table 1.

X-Ray Diffraction (XRD) Analysis

The powdered sample was dried in an oven at 105°C for 24 hours to remove moisture. A small amount (0.5-1.0 g) of the dried powder was evenly distributed on a sample holder and smoothed to achieve a flat surface. The XRD instrument was calibrated using a standard reference material to ensure accurate results. The sample holder was then placed in the XRD chamber, and the X-ray tube was set to an optimal voltage (30-50 kV) and current (10-40 mA). The X-ray diffraction pattern was obtained by scanning the sample over a 2θ range of 5-60°, with a step size of 0.02° and a scan speed of 1°/min. The analysis was conducted in accordance with ISO 18325:2016 and the result is depicted as shown in Figure 2.

Preparation of Rice Husk (RH) and Sugarcane Bagasse (SCB)

The RH and SCB were subjected to a series of preparation steps. Initially, they were washed with clean water to remove contaminants and then dried in an oven at 150°C. The dried fibers were then pulverized in a ball mill at 300 rpm for 1 hour, followed by sieving to obtain particles with a size of ≤300 μm, as previously described (Dele-Afolabi et al., 2018).

Thermogravimetric Analysis (TGA/DTG)

The RH and SCB samples were ground into a fine powder to ensure uniformity. Approximately 5-10 mg of each sample was weighed using an analytical balance and placed in a clean, dry platinum or alumina crucible. The

Corresponding author: Yusuf Tijjani
ytijjani.mec@buk.edu.ng
Department of Mechanical Engineering, Bayero University Kano, Kano State, Nigeria.

JOURNAL OF SCIENCE TECHNOLOGY AND EDUCATION 13(1), MARCH, 2025
ISSN: 2277-0011; Journal homepage: www.atbuftejoste.com.ng

TGA/DTG analysis was conducted in air atmosphere, simulating real-world combustion conditions, over a temperature range of 25°C to 900°C at a heating rate of 10°C/min. Prior to analysis, the TGA/DTG system was calibrated with standard materials to ensure accurate temperature and weight measurements. The samples were carefully loaded into the sample holder, and the analysis was initiated using the instrument's software interface. The curves are depicted in the Figures 3 and 4.

Preparation of Porous Ceramics

Dense and porous ceramics were fabricated using a formulation consisting of $Al_2O_32SiO_2.2H_20$·– xPFAs (x = 0, 3, 6, and 9 wt%), where RH and SCB served as pore formers, 20 wt% bentonite clay as a binder, and water. The kaolin powder and pore formers (RH or SCB) were dry milled for 1 hour at 200 rpm to obtain a homogeneous mixture. Bentonite clay and water were then added, and the mixture was pressed into green pellets using a 25 mm diameter ceramic die. The pellets were air-dried for 2 days and oven-dried at 150°C for 2 hours. The samples were then heated to 700°C for 2 hours to burn out the fibers, followed by sintering at 1100°C for 2 hours to consolidate the porous ceramic structure. This procedure was adapted from a previous study (Dele-Afolabi et al., 2021). The schematic diagram for the production of porous kaolin ceramic samples is as depicted in Figure below.

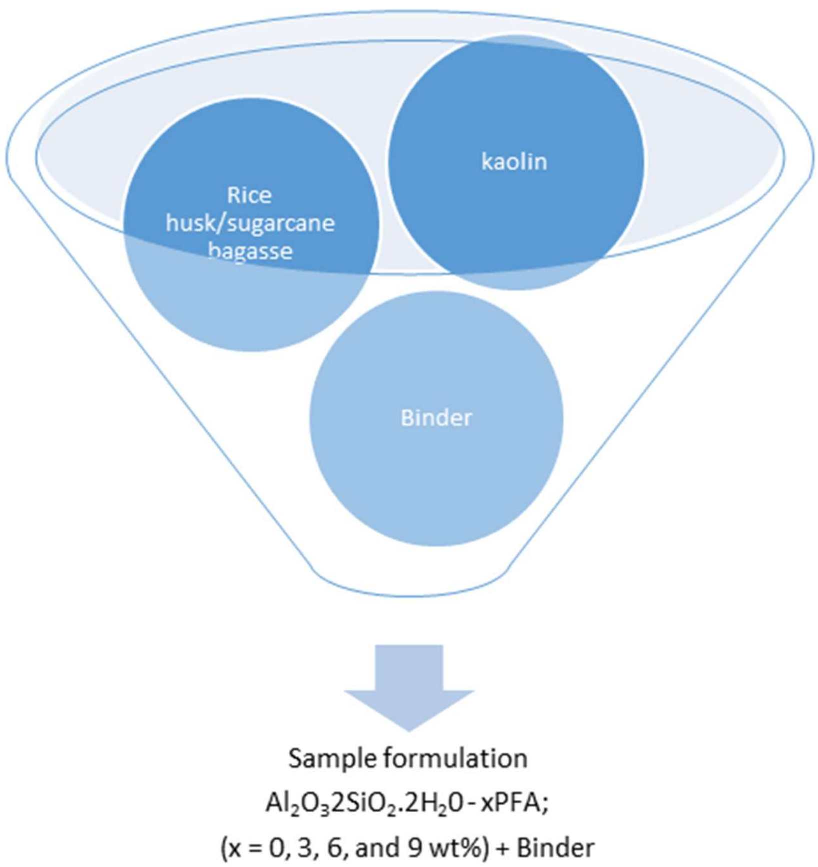

Corresponding author: Yusuf Tijjani
ytijjani.mec@buk.edu.ng
Department of Mechanical Engineering, Bayero University Kano, Kano State, Nigeria.

JOURNAL OF SCIENCE TECHNOLOGY AND EDUCATION 13(1), MARCH, 2025
ISSN: 2277-0011; Journal homepage: www.atbuftejoste.com.ng

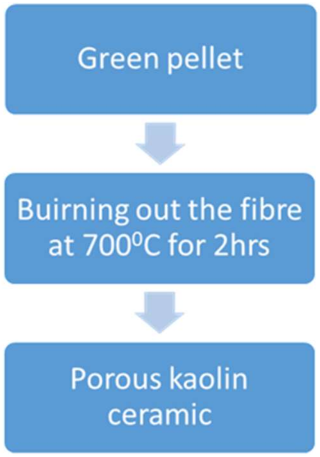

Figure 2: Block diagram for the production of kaolin ceramic samples

Density and Porosity Measurements

The density and porosity of the sintered ceramic samples were determined using Archimedes' method (ASTM C20-00). The measurements involved determining the mass of the dry sample (W_1) and the mass of the sample submerged in water (W_2). The volume of the solid ceramic material V_{solid} was calculated using the equation:

$$V_{solid} = \frac{W_1 - W_2}{\rho_{liquid}}$$

where ρ_{liquid} is the density of water (approximately 1 g/cm³). The total volume of the sample, including pores, was determined by the volume of liquid displaced when the sample was submerged. From these measurements, the density, open porosity, and total porosity of the samples were calculated. The porosities of the samples measured are depicted in Table 2

Scanning Electron Microscope (SEM) images

The microstructure of the porous ceramic samples was investigated using scanning electron microscopy (SEM). SEM images of samples containing 3%, 6%, and 9% RH and SCB were analyzed, revealing the presence of intentionally introduced porosities. The images were captured at as depicted in Figure 5, allowing for a detailed examination of the pore structure. The average pore size diameters were quantified using ImageJ micrograph image analysis tool, providing valuable insights into the microstructural characteristics of the samples.

RESULTS AND DISCUSSION

X- Ray Fluorescence (XRF) Result of the Kaolin Powder

Table 1: Oxides composition of Gwarzo kaolin.

Oxides	SiO2	Al2O3	TiO2	Fe2O3	SO3	CaO	K2O	Cl	ZrO2
Percentage composition	53.96	37.94	3.14	1.65	0.48	0.33	1.06	0.68	0.22

The oxide composition of the Gwarzo kaolin, presented in Table 1 above, reveals a significant presence of silica (53.9%) and alumina (37.94%), along with other impurities. These results are consistent with the theoretical composition of kaolinite, which typically comprises approximately 46.5% silicon oxide (SiO_2) and 39.5% alumina (Al_2O_3). The similarity between the observed composition and the theoretical values, as well as with other kaolin clays reported globally, suggests that the Gwarzo kaolin conforms to the characteristic mineralogical profile of kaolinite.

Corresponding author: Yusuf Tijjani
ytijjani.mec@buk.edu.ng
Department of Mechanical Engineering, Bayero University Kano, Kano State, Nigeria.

JOURNAL OF SCIENCE TECHNOLOGY AND EDUCATION 13(1), MARCH, 2025
ISSN: 2277-0011; Journal homepage: www.atbuftejoste.com.ng

X-Ray Diffraction Result of the clay (Kaolin powder)

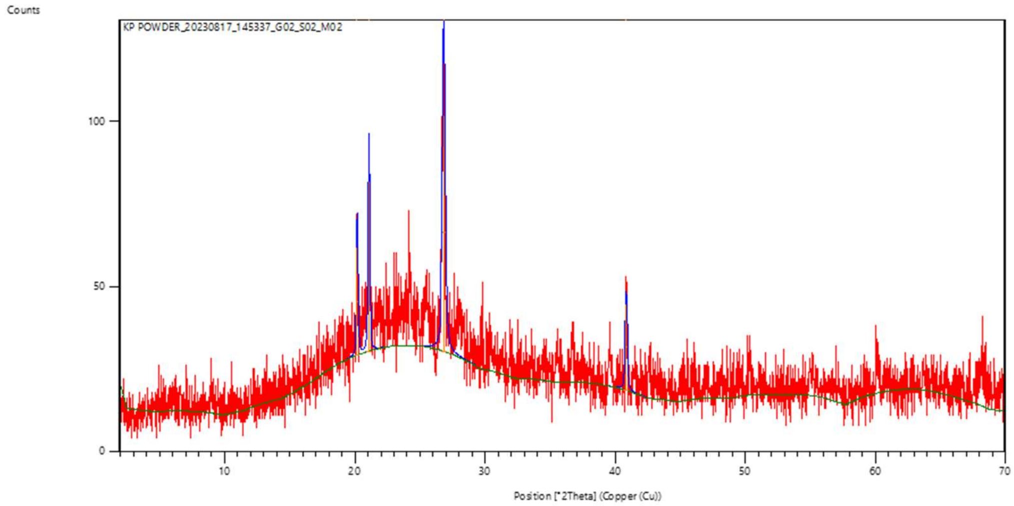

Figure 2: Phase view of the powder obtained from XRD.

The X-ray diffraction (XRD) pattern of the kaolin sample, presented in Figure 2, exhibits a prominent peak at 26.8° (2θ), which is consistent with the crystallographic plane of kaolinite (JCPDS 14-164) at 26.6° (2θ). Additionally, the XRD spectrum reveals the presence of quartz (JCPDS 46-1045) and silica, indicating the mineralogical composition of the kaolin sample.

Thermal Analysis of Rice Husk (RH) and Sugarcane Bagasse (SCB)

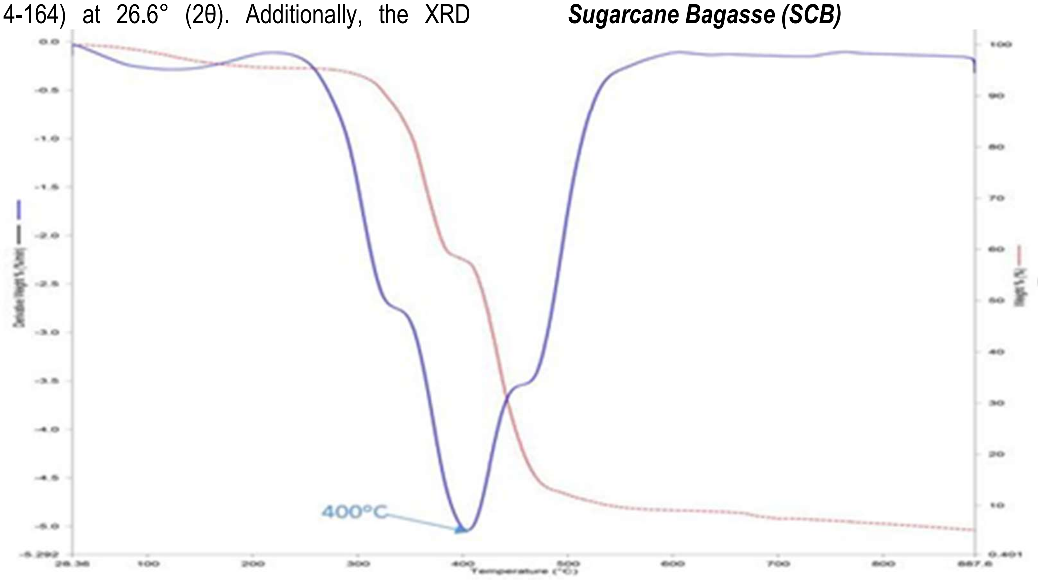

Figure 3: Thermogravimetric/Differential Thermogravimetry curves of RH

Corresponding author: Yusuf Tijjani
ytijjani.mec@buk.edu.ng
Department of Mechanical Engineering, Bayero University Kano, Kano State, Nigeria.

JOURNAL OF SCIENCE TECHNOLOGY AND EDUCATION 13(1), MARCH, 2025
ISSN: 2277-0011; Journal homepage: www.atbuftejoste.com.ng

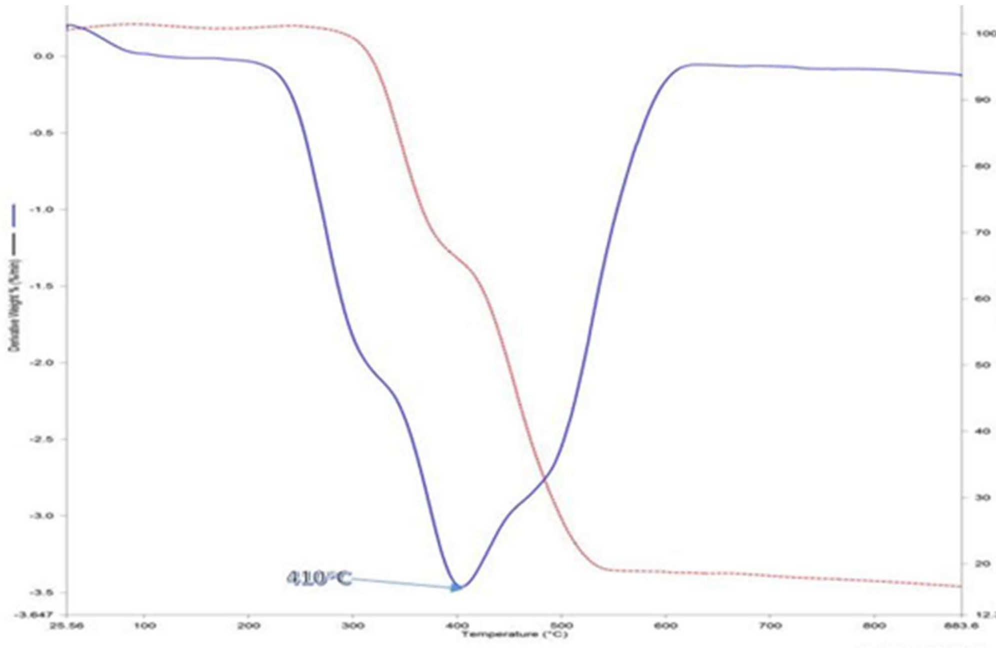

Figure 4: Thermogravimetric/Differential Thermogravimetry curves of SCB

The thermal behavior of the pore formers, RH and SCB, was investigated using thermogravimetric analysis (TGA) and differential thermogravimetric analysis (DTG). The TGA and DTG curves, presented in Figures 3 and 4, respectively, show similar trends for both RH and SCB. The initial weight loss between 30°C and 150°C is attributed to the removal of physically bonded water. Subsequent decomposition of hemicellulose and cellulose, followed by lignin, was observed at higher temperatures. The decomposition temperatures varied between the two pore formers, with RH decomposing between 320°C and 600°C, exhibiting an endothermic peak at approximately 400°C. In contrast, SCB showed an endothermic peak around 410°C. These results informed the development of a heating schedule for the porous kaolin samples.

Porosity and Density of Samples

Table 2: Summary of sample formulation, and their corresponding average pore sizes, densities and porosity parameters

Pore former type	Content	Average pore size diameter (µm)	Density (g/cm3)	Open porosity	Average pore size diameter (µm)
RH	0	6.99	1.3	22	38.2
	3	14.45	1.07	37	64.5
	6	16.33	1.03	39.8	57.3
	9	20.32	1.003	40.3	48.7
SCB	0	6.99	1.3	22	38.2
	3	16.33	1.03	38.2	56.6
	6	22.88	0.995	41.9	45.5
	9	49.24	0.94	44.6	-

Corresponding author: Yusuf Tijjani
ytijjani.mec@buk.edu.ng
Department of Mechanical Engineering, Bayero University Kano, Kano State, Nigeria.

JOURNAL OF SCIENCE TECHNOLOGY AND EDUCATION 13(1), MARCH, 2025
ISSN: 2277-0011; Journal homepage: www.atbuftejoste.com.ng

Morphology of the Porous Ceramic Samples

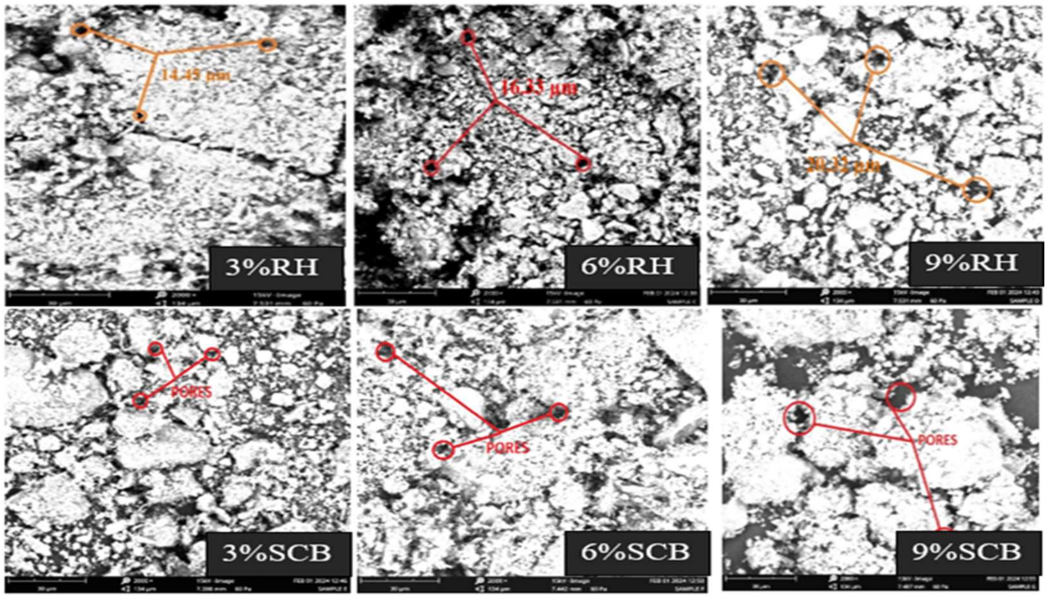

Figure 5: SEM Micrographs of Porous RH and SCB Ceramics, Magnification: 30μm

Based on the Table 2 and Figure 5 above the following parameters can be discussed as follows:

Average Pore Size Diameter

The average pore size diameter was determined using ImageJ micrograph image analysis tool, which analyzed the SEM images of the ceramic samples. The results showed that the average pore size diameter increased with the weight percentage of both RH and SCB pore formers. For RH, the average pore size increased gradually from 14.45 µm to 20.32 µm as the RH content increased from 3% to 9%. In contrast, SCB resulted in a more significant increase in average pore size, reaching 49.24 µm at 9% SCB content. The SEM images revealed a uniform distribution of pores in the ceramic matrix, with the pores becoming larger and more irregular as the pore former content increased. The ImageJ analysis tool enabled the quantification of the pore size distribution, which was essential for understanding the microstructure of the ceramic samples.

The difference in pore size can be attributed to the physical and chemical characteristics of the pore formers, with RH producing smaller, more uniform pores due to its finer particles and higher silica content (Dele-Afolabi *et al.,* 2018). Similar findings have been reported in previous studies, where the pore size distribution was influenced by the type and content of pore formers (Shukor *et al.,* 2024). The SEM images also showed that the pores were well-distributed and interconnected, which is essential for achieving the desired properties in porous ceramics.

Density

The density of the porous ceramic samples decreased as the weight percentage of both RH and SCB pore formers increased. For RH, the density decreased gradually from 1.07 g/cm³ to 1.003 g/cm³ as the RH content increased from 3% to 9%. In contrast, SCB resulted in a more rapid decrease in density, reaching 0.94 g/cm³ at 9% SCB content. The greater decrease in density for SCB samples can be attributed to the larger and more irregular pores created by SCB, as observed in the SEM images. This trend is consistent with previous studies, which have

Corresponding author: Yusuf Tijjani
ytijjani.mec@buk.edu.ng
Department of Mechanical Engineering, Bayero University Kano, Kano State, Nigeria.

JOURNAL OF SCIENCE TECHNOLOGY AND EDUCATION 13(1), MARCH, 2025
ISSN: 2277-0011; Journal homepage: www.atbuftejoste.com.ng

reported a decrease in density with increasing pore former content (Agbo *et al.,* 2015).

Open Porosity

The open porosity of the ceramic samples increased with the weight percentage of both RH and SCB pore formers. SCB showed a consistently higher porosity than RH at all weight percentages, with a more substantial increase in porosity across the range. This suggests that SCB is more effective at creating voids in the ceramic, potentially due to its fibrous structure and higher cellulose content.

Total Porosity

The total porosity of the ceramic samples also increased with the weight percentage of both RH and SCB pore formers. The increase in porosity resulted in a decrease in the material's density, as the volume of solid material was replaced by voids introduced by the pore formers.

CONCLUSION

In conclusion, the incorporation of RH and SCB as pore formers in kaolin ceramics significantly enhances porosity while reducing density. The density decrease is more gradual with RH, resulting in denser ceramics compared to SCB equivalent proportions, potentially due to the complementary silica content in the kaolin/RH sintered ceramic. The porosity and pore diameter measurements suggest that Gwarzo kaolin is a promising material for fabricating macro-filters suitable for initial water treatment stages. Both rice husk and sugarcane bagasse can be effective pore formers, depending on the desired porosity level. These findings are consistent with established pore size classifications, indicating the potential of these materials for various applications.

REFERENCES

Abdullayev, A., Bekheet, M. F., Hanaor, D. A., & Gurlo, A. (2019). Materials and applications for low-cost ceramic membranes. *Membranes*, *9*(9), 105.

Agbo, S. C., Ekpunobi, E. U., Onu, C. C., & Akpomie, K. G. (2015). Development of Ceramic Filter Candle from NSU (Kaolinite Clay) for Household Water Treatment. International Journal of Multidisciplinary Sciences and Engineering, 6(10), 18–23.

Aissat, M., Hamouda, S., Bettahar, N., Tarboush, B. A., & Bahmani, A. (2019). Characterization and application of ceramic membranes prepared from Algerian kaolin. *Cerâmica*, *65*(376), 554-561.

Ali, M. B., Hamdi, N., Rodriguez, M. A., Mahmoudi, K., & Srasra, E. (2018). Preparation and characterization of new ceramic membranes for ultrafiltration. *Ceramics International*, *44*(2), 2328-2335.

American Society for Testing and Materials. (2010). ASTM C20-00 (2010): Standard test methods for apparent porosity, water absorption, apparent specific gravity, and bulk density of burned refractory brick and shapes by boiling water. *Refract Stand*, *15*,1-3.

Chindaprasirt, P., Kanchanda, P., Sathonsaowaphak, A., & Cao, H. T. (2007). Sulfate resistance of blended cements containing fly ash and rice husk ash. *Construction and Building Materials*, *21*(6), 1356-1361.

Christophe, C., Philippe, A., Guérin, G., Mercier, N., & Guibert, P. (2018). Bayesian approach to OSL dating of poorly bleached sediment samples: Mixture Distribution Models for Dose (MD2). *Radiation Measurements*, *108*, 59-73.

Dele-Afolabi, T., Mohamed Ariff, A. H., Mazlan, N., Sobri, S., Calin, R., & Zahari Nur, I. (2018). Effect of agro-waste pore formers on the microstructure, hardness, and tensile properties of porous alumina ceramics. *International Journal of Applied Ceramic Technology*, *15*(4), 1060-1071.

Corresponding author: Yusuf Tijjani
ytijjani.mec@buk.edu.ng
Department of Mechanical Engineering, Bayero University Kano, Kano State, Nigeria.

JOURNAL OF SCIENCE TECHNOLOGY AND EDUCATION 13(1), MARCH, 2025
ISSN: 2277-0011; Journal homepage: www.atbuftejoste.com.ng

Dele-Afolabi, T. T., Azmah Hanim, M. A., Jung, D. W., Ilyas, R. A., Calin, R., & Nurul Izzah, A. R. (2022). Rice Husk as a Pore-Forming Agent: Impact of Particle Size on the Porosity and Diametral Tensile Strength of Porous Alumina Ceramics. *Coatings*, *12*(9), 1259.

Dhuban, S. B., Ramesh, S., Tan, C. Y., Wong, Y. H., Alengaram, U. J., Teng, W. D., ... & Sutharsini, U. (2019). Sintering behaviour and properties of manganese-doped alumina. *Ceramics international*, *45*(6), 7049-7054.

Haghdan, S., Renneckar, S., & Smith, G. D. (2016). Lignin in Polymer Composites. *Journal and Books*, 1-11.

Hubadillah, S. K., Othman, M. H. D., Tai, Z. S., Jamalludin, M. R., Yusuf, N. K., Ahmad, A., ... & Harun, Z. (2020). Novel hydroxyapatite-based bio-ceramic hollow fiber membrane derived from waste cow bone for textile wastewater treatment. *Chemical Engineering Journal*, *379*, 122396.

Kamoun, N., Jamoussi, F., & Rodríguez, M. A. (2020). The preparation of meso-porous membranes from Tunisian clay. *boletín de la sociedad española de cerámica y vidrio*, *59*(1), 25-30.

Li, L., Cao, G., Zhao, R., Wu, S., Wang, L., Li, X., & Zeng, S. (2020). Recycling of construction and demolition waste to fabricate cost-effective anorthite ceramic membranes for enhanced separation of an oil-in-water emulsion. *Construction and Building Materials*, *265*, 120512.

Li, D., & Li, M. (2012). Porous Y2SiO5 ceramic with low thermal conductivity. *Journal of Materials Science & Technology*, *28*(9), 799-802.

Lima, L. K., Santana, L. N., Lira, H. L., Rodríguez, M. A., Souza, M. Y., Júnior, M. G., & Lira, B. S. (2024). Development of asymmetric ceramic membranes for dairy wastewater treatment–A comparison between co-sintering and conventional firing process. *Journal of Water Process Engineering*, *57*, 104611.

Mohanta, K., Kumar, A., Parkash, O., & Kumar, D. (2014). Processing and properties of low-cost macroporous alumina ceramics with tailored porosity and pore size fabricated using rice husk and sucrose. *Journal of the European Ceramic Society*, *34*(10), 2401-2412.

Ohji, T., & Fukushima, M. (2012). Macro-porous ceramics: processing and properties. *International Materials Reviews*, *57*(2), 115-131.

Phonphuak, N., & Chindaprasirt, P. (2015). Types of waste, properties, and durability of pore-forming waste-based fired masonry bricks. *Eco-efficient masonry bricks and blocks*, 103-127.

Ren, D., Colosi, L. M., & Smith, J. A. (2013). Evaluating the sustainability of ceramic filters for point-of-use drinking water treatment. *Environmental Science & Technology*, *47*(19), 11206-11213.

Roohani-Esfahani, S. I., Chen, Y., Shi, J., & Zreiqat, H. (2013). Fabrication and characterization of a new, strong and bioactive ceramic scaffold for bone regeneration. *Materials Letters*, *107*, 378-381.

Saini, P., Bulasara, V. K., & Reddy, A. S. (2019). Performance of a new ceramic microfiltration membrane based on kaolin in textile industry wastewater treatment. *Chemical Engineering Communications*, *206*(2), 227-236.

Shukor, M. S. S. A., Ahmad, S., Muslem, M. F., Rahman, H. A., Mahzan, S., Jaidi, Z., & Noor, F. M. (2024). Fabrication Of Silica Water Filter From Rice Husk Waste Product Via Slip Casting Method. *Malaysian Journal of Microscopy*, *20*(1), 74-84.

Souza, M. Y. M. D., Lira, H. D. L., Santana, L. N. D. L., & Rodríguez, M. A. (2021). Preparation and application in crude oil-water separation of clay-based membranes. *Materials Research*, *24*(4), e20200508.

Corresponding author: Yusuf Tijjani
ytijjani.mec@buk.edu.ng
Department of Mechanical Engineering, Bayero University Kano, Kano State, Nigeria.

Wei, G. U. O., Hongbin, L. U., & Chunxia, F. E. N. G. (2010). Influence of La2O3 on preparation and performance of porous cordierite from rice husk. *Journal of rare earths*, *28*(4), 614-617.

Xavier, L. A., Fetzer, D. E. L., de Oliveira, T. V., Eiras, D., Voll, F. A. P., & Vieira, R. B. (2022). Effect of stainless-steel slag concentration in the fabrication of cost-effective ceramic membranes: Seawater pre-treatment application. *Ceramics International*, *48*(16), 23273-23283.

Yang, Z., Yin, Z., Wang, D., Wang, H., Song, H., Zhao, Z., ... & Jin, H. (2020). Effects of ternary sintering aids and sintering parameters on properties of alumina ceramics based on orthogonal test method. *Materials Chemistry and Physics*, *241*, 122453.

Zewdie, T. M., Prihatiningtyas, I., Dutta, A., Habtu, N. G., & Van der Bruggen, B. (2021). Characterization and beneficiation of Ethiopian kaolin for use in fabrication of ceramic membrane. *Materials Research Express*, *8*(11), 115201.

Zou, J., Dai, Q., Zhou, X., Qin, H., Guo, W., Gao, P., & Xiao, H. (2024). Preparation of alumina disc ceramic membrane with enhanced abrasion resistance for dynamic membrane filtration. *Ceramics International*, *50*(6), 9354-9362.

Corresponding author: Yusuf Tijjani
ytijjani.mec@buk.edu.ng
Department of Mechanical Engineering, Bayero University Kano, Kano State, Nigeria.